PHYSICAL REVIEW A **74**, 012723 (2006)

Collision-induced spectroscopy with long-range intermolecular interactions: A diagrammatic representation and the invariant form of the induced properties

A. P. Kouzov[*]
Institute of Physics, Saint Petersburg State University, Ulyanovskaya str. 1, Peterhof, Saint Petersburg 195904, Russia

M. Chrysos,[†] F. Rachet, and N. I. Egorova[‡]
Laboratoire des Propriétés Optiques des Matériaux et Applications,
UMR CNRS 6136, Université d'Angers, 2 boulevard Lavoisier, 49045 Angers, France
(Received 9 March 2006; published 31 July 2006)

Collision-induced properties of two interacting molecules *a* and *b* are derived by means of a general diagrammatic method involving *M* molecule-molecule and *N* photon-molecule couplings. The method is an extension of previous graphical treatments of nonlinear optics because it exhaustively determines interaction-induced polarization mechanisms in a trustworthy and handy fashion. Here we focus on long-range intermolecular interactions. Retardation effects are neglected. A fully quantum-mechanical treatment of the molecules is made whereas second quantization for the electromagnetic field, in the nonrelativistic approximation, is implicitly applied. The collision-induced absorption, Raman, and hyper-Raman processes are viewed and studied, through guiding examples, as specific cases $N=1$, 2, and 3, respectively. In Raman ($N=2$), the standard first-order ($M=1$) dipole-induced dipole term of the incremental polarizability, $\Delta\hat{\alpha}$, is the result of a coupling of the two photons with distinct molecules, *a* and *b*, which perturb each other via a dipole-dipole mechanism. Rather, when the two photons interact with the same molecule, *a* or *b*, the ($N=2$, $M=1$) graphs predict the occurrence of a nonlinear polarization mechanism. The latter is expected to contribute substantially to the collision-induced Raman bands by certain molecular gases.

DOI: 10.1103/PhysRevA.74.012723 PACS number(s): 34.90.+q, 33.20.Ea, 42.65.An, 33.20.Fb

I. INTRODUCTION

Collision-induced absorption (CIA) and Raman scattering (CIRS) have contributed much over the past 25 years to the comprehension of the intermolecular interactions and dynamics of the relative translational motion, in either gaseous, liquid, or solid-state phases [1–3]. The experimental achievements have helped to develop sophisticated multidimensional surfaces of the incremental binary dipole moments $\Delta\boldsymbol{\mu}$ and polarizabilities $\Delta\hat{\alpha}$, these quantities being of primary importance to CIA and CIRS. As $\Delta\boldsymbol{\mu}$ and $\Delta\hat{\alpha}$ are often related to properties of isolated molecules, CIA and CIRS spectroscopy have substantially added to molecular electro-optics, providing its literature with data [4–7] that other techniques are hardly able (if at all) to obtain. Moreover, the quantities so accessed serve as a touchstone for quantum chemistry methods.

In most of the molecular systems of practical importance, such spectra are fingerprints of the long-range induction [1,2,4–8] (and references therein). Although it is of widespread use to model those interactions with classical physics, classical modeling has the serious drawback of a lack of systematics. Specifically, when refinements are required, it is unable to guarantee the extensibility of the derived corrections; in addition, the description of the behavior of some frequency-dependent molecular properties may encounter problems, especially in preresonance situations.

Aside from the extensive theoretical and experimental studies on collision-induced Raman scattering (CIRS), recently, collision-induced hyper-Raman scattering (CIHRS) was detected in the liquid phase [9]. This process, and the concomitant spectra, is the signature of incremental second-order hyperpolarizabilities $\Delta\hat{\beta}$. However, the problem of the interpretation of the recorded profile remains open because it requires a good knowledge of $\Delta\hat{\beta}$. The modeling of this property and the way it should enter the calculation is far more delicate than the modeling of $\Delta\hat{\alpha}$ and constitutes a topic at issue [10,11] (and references therein). Clearly, the need to develop a universal tool, capable of treating exactly (that is, quantum mechanically) the long-range intermolecular polarization, becomes more than timely.

The aforementioned problems have much in common with those encountered in interactions of a nonlinearly polarized free molecule with an electromagnetic field. To solve the latter, an effective diagrammatic method has been developed [12–14], which has found numerous applications in nonlinear optics [15] and has strongly boosted its progress.

Here, the diagrammatic method is generalized to tackle the collision-induced polarization mechanisms in a pair of interacting molecules *a* and *b*. Although the problem of the graphical representation of a molecular pair interacting with photons has been addressed in the past with QED [16], the previous study has been restricted to interaction energies, that is, to properties of a lower complexity than the ones treated here.

In the framework of our approach, a fully quantum-mechanical treatment for the molecules is made and a quantized radiative field is implicitly employed. The intermolecu-

---

[*] Email address: alex@AK1197.spb.edu

[†] Email address: michel.chrysos@univ-angers.fr

[‡] Also at Institute of Physics, Saint Petersburg State University, Ulyanovskaya Str. 1, Peterhof, Saint Petersburg 195904, Russia.

lar separation, R, is assumed to satisfy $R_0 \ll R \ll \lambda_L$, where R_0 and λ_L denote the typical overlap range and the laser wavelength, respectively. In this regime, solely the long-range intermolecular interactions are relevant, whereas the nonrelativistic treatment of the field is fully justified by the neglect of any retardation effects. Furthermore, we implicitly assume that both molecule-molecule and molecule-field interactions are weak enough so that perturbation theory is applicable. Provided that the latter assumption remains valid, our approach is straightforwardly extensible to trimers or to clusters.

Our method, accounting for the exact quantum-mechanical spectral decomposition of the transition amplitude over the supermolecule-plus-field eigenstates, is able to specify, classify, and depict the collision-induced polarization mechanisms in a reliable, exhaustive, and handy fashion, a task that classical theory is unable to accomplish. Then, by using frame-independent expressions of the long-range potential [17], the method can be combined with the irreducible spherical tensor (IST) approach [18] to provide binary incremental properties at will. Guiding examples of how to decouple the field from the intermolecular properties in the transition amplitude are given. In so doing, expressions for these properties are simultaneously cast into an invariant form.

II. FEYNMAN DIAGRAMS

A. Light absorption and scattering by a single molecule

In interactions between a molecule and the electromagnetic field, the molecule undergoes a transition $f \leftarrow i$ from its initial state i to a final state f. To the N perturbation order, the transition amplitude U_N is given by the concomitant matrix element of the coupling between the molecule and the quantized field, and can be depicted by a set of $N!$ Feynman diagrams that help to represent the various coupling sequences $n=1,2,\ldots,N$ between the molecule and the photons [12–16]. Aside from the aforementioned assumption that perturbation theory holds, henceforward we further assume that: the field amplitudes can be dissociated from U_N so that the latter contains only the unit polarization vectors (standard factors depending on the matrix elements of the photon creation and annihilation operators are also dropped from U_N); the Born-Oppenheimer approximation holds, and the $f \leftarrow i$ transition occurs within the ground electronic state. Under these assumptions, U_N is proportional to the rotovibrational matrix element of the $(N-1)$th-order nonlinear polarizability in scalar form [15]. The energy conservation law reads $\omega_{fi} = \Sigma_{n=1}^{N} \pm \omega_n$, where $\omega_{fi} = (E_f - E_i)/\hbar$ is the frequency of the transition undergone by the molecule, E_i (E_f) is the energy of the initial (final) state, and $\omega_n (>0)$ is the frequency of the nth absorbed or emitted photon. To fully specify and distinguish absorbed and emitted photons, their frequencies are supplied with a sign, $\pm\omega_n$, and their polarization vectors are defined as complex conjugated quantities, $\mathbf{e}_n$ and $\mathbf{e}_n^*$, respectively. For scattering, N will always correspond to spontaneous emission, where part of the field energy is converted to excitations of the molecule. As conventionally adopted, the molecule-dipole field couplings are expressed as scalar products $V_n = -(\mathbf{e}_n, \boldsymbol{\mu})$ of the photon polarization vectors with the dipole moment operator. In a typical graph, V_n are represented by vertices, and photons are depicted by incoming (absorption) and outgoing arrows (emission) crossing the vertex. Whenever a vertex is crossed, a factor appears in the spectral expansion of U_N. For $n < N$, this factor is the ratio of the matrix element $(V_n)_{k'k}$[19] (k and k' being virtual states emerging before and after the V_n vertex crossing, respectively) by the energy difference between the initial "molecule-plus-field" state and the one emerging once the interaction V_n has been completed (see, for instance, [12,13]). For the last vertex ($n=N$), the factor is given as the matrix element $(V_n)_{fk}$ alone. To represent virtual states in the spectral expansion of U_N, the basis of the exact molecular eigenvectors is used.

Accordingly, in single-photon absorption, the amplitude is $U_1 = -(\mathbf{e}_1, \boldsymbol{\mu})_{fi}$. This is shown in Fig. 1(a). Rather, for Raman scattering, there are two possible sequences contributing to the scattering amplitude U_2. These are depicted by the two-photon graphs of Figs. 1(b) and 1(c). In Fig. 1(b), the photon 1 is first absorbed and then the photon 2 is emitted. In Fig. 1(c), absorption and emission are interchanged in time. The corresponding terms are

$$U_2^{\mathrm{b}} = \sum\nolimits_k (\hbar\omega_{ki} - \hbar\omega_1)^{-1} (\mathbf{e}_1, \boldsymbol{\mu})_{ki} (\mathbf{e}_2^*, \boldsymbol{\mu})_{fk},$$

$$U_2^{\mathrm{c}} = \sum\nolimits_k (\hbar\omega_{ki} + \hbar\omega_2)^{-1} (\mathbf{e}_2^*, \boldsymbol{\mu})_{ki} (\mathbf{e}_1, \boldsymbol{\mu})_{fk},$$

where superscripts "b" and "c" denote the corresponding panels of Fig. 1.

B. Collision-induced processes by a pair of interacting molecules

We now turn our attention to the problem of a pair of neutral molecules a and b that are simultaneously perturbed both by a sequence of molecule-dipole field couplings V_n ($n=1,2,\ldots,N$) and by a sequence of intermolecular couplings W_m ($m=1,2,\ldots,M$). Analogously to N and n, the role of the subscripts M and m (here introduced) is to specify, within perturbation theory, the order of the intermolecular interaction in the analysis. Let I and F be the initial and final states of the a-b pair. We assume that I and F have a common electronic part and that the constituent molecules are in their ground electronic state. We point out that this assumption is not at all a restriction of the generality of the theory, which is equally applicable to collision-induced vibronic effects. Rather, it is made by the convenience of matching the working conditions of experiments in the current state of the art, namely, experiments focusing on spectra of collision-induced pure vibrational transitions.

By contrast with the single molecule problem, here we are concerned with some extended amplitude $U_{N,M}$, due to states I and F and to both types of coupling. The amplitude must be calculated off the vibronic energy shell, the quantity $\hbar(\omega_{FI} - \Sigma_{n=1}^{N} \pm \omega_n)$ now amounting precisely to the rototranslational energy defect. In a two-molecule Feynman graph,

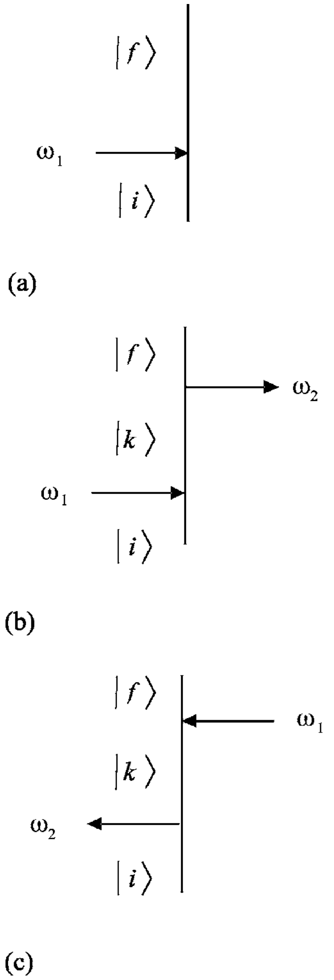

FIG. 1. Typical one-line graphs used to depict distinct spectroscopic processes for an isolated molecule. (a) Single-photon absorption ($N=1$). The molecule absorbs photon ω_1, and switches from state $|i\rangle$ to state $|f\rangle$. (b),(c) Raman scattering ($N=2$). The molecule switches from $|i\rangle$ to $|f\rangle$ via virtual intermediate states $|k\rangle$ that interpose themselves within the time-ordered sequence absorption-emission (b) or the reverse (c). Note that scenarios (b) and (c) are indistinguishable in practice and they both interfere to the Raman scattering amplitude.

the state of a-b is depicted by a pair of time-ordered vertical lines, each representing the evolution of a specific molecule. An arrow, depicting single-photon absorption or emission, is free to be attached to any of the lines. Its presence alters the state of the corresponding molecule (see also [16]). The action of W is depicted by M horizontal segments with vertices at lines a and b. At vertices, both molecules change states. By contrast with the single molecule problem, here it is preferable not to use the exact eigenvectors of the pair, since the rototranslational states are in most cases strongly coupled by W. Rather, the rototranslational configuration is kept frozen and full advantage of the vibronic wave functions as a basis is taken. Given that, in general, intermolecular forces only weakly perturb vibrational spectra, a rapidly converging perturbation series is obtained. Furthermore, we assume the rototranslational motion to be slow compared to the molecular vibrations. The resulting vibrational amplitude $U_{N,M}$ is a function of the rototranslational geometry, and the relevant incremental electro-optic properties can be derived.

Overlap effects are assumed to be negligible. With this assumption, any additional mixing of the electronic wave functions of different molecules caused by the Pauli's exclusion principle can be disregarded, while in addition, the study can be restricted to easily polarizable particles for which long-range interactions are predominant. In this way, the frame-independent expansion of $W=\Sigma_{l_a l_b} W_{l_a l_b}$ [17] over the multipole-multipole interactions can be worked upon, allowing us to determine the role of the constituent terms as well as to put the final results in an invariant form. The IST technique [18] turns out to be the most suitable device to attain this object.

1. Light absorption

a. First-order effects ($M=1$). In general, when the photon has been absorbed and the collision has been completed, it is likely that both molecules have switched from vibrational states i_c to states f_c ($c=a,b$). This is referred to as the *simultaneous transition* or the *double transition*. Using Feynman diagram conventions for the perturbative matrix elements, one gets

$$U_{1,1} = \frac{1}{\hbar}\sum_{k_a}\left(\frac{\langle k_a \mid (\mathbf{e},\boldsymbol{\mu}_a)|i_a\rangle\langle f_a f_b|W_{l_a l_b}|k_a i_b\rangle}{\omega_{k_a i_a}-\omega} + \frac{\langle k_a f_b|W_{l_a l_b}|i_a i_b\rangle\langle f_a|(\mathbf{e},\boldsymbol{\mu}_a)|k_a\rangle}{\omega_{k_a i_a}+\omega_{f_b i_b}}\right). \tag{1}$$

The two terms in parentheses correspond to the first and second graphs of Fig. 2, respectively, depicting absorption of a photon by molecule a. The lowest multipolar rank l_b is defined by the symmetry of the constituent states of molecule b, which plays the role of the inductor. The longest-range dipole-field induction, $U_{1,1}\propto R^{-3}$, arises at $l_b=1$ when a dipole moment is excited by the vibration. There exist two analogous graphs (not shown) for photon absorption by molecule b.

Obviously, when b is a (neutral) atom remaining in its S state throughout the process, the graphs of Fig. 2 produce no amplitude. In this case, solely two diagrams contribute to light absorption, both having photon arrows ending at line b. Of course, a nonzero transition probability implies that molecule a has a nonvanishing transition multipole.

b. Second-order effects ($M=2$). When the sets l_a, l_b and l'_a, l'_b of the multipolar ranks (used to specify the interactions) differ from one another, we obtain $3!=6$ diagrams depicting photon absorption by molecule a. For the leading term, the relevant intermolecular couplings are W_{21} and W_{11}. This corresponds to dispersion induction and scales like R^{-7}. Figure 3 shows a typical graph of this group of diagrams. There are another six diagrams (not shown) contributing to the dispersion polarization with as couplings W_{12} and W_{11} and with the photon arrow ending at line b. Here, unlike $M=1$, a nonzero dipole moment is induced even when two dissimilar S-state atoms are involved in the encounter.

In the remainder of this paper, the state vectors have been

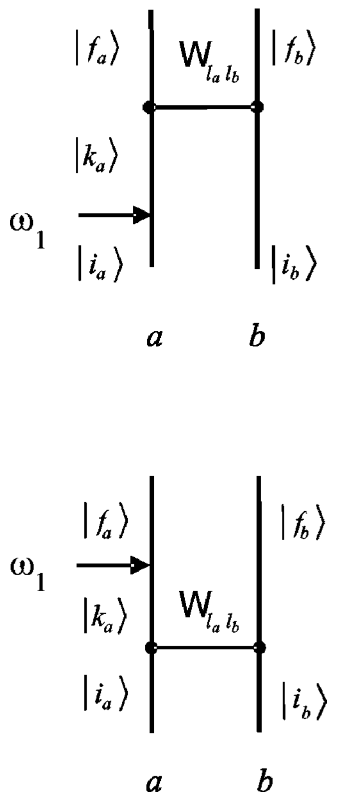

FIG. 2. Collision-induced absorption. The process implicates one photon ($N=1$) and two molecules *a* and *b*. To the first order, a single intermolecular coupling is involved ($M=1$), depicted by a segment to interconnect the vertical lines. There are two graphs relevant to this process with the photon absorbed by the same molecule (here, *a*), because the intermolecular coupling may follow or precede the molecule-dipole field coupling. In either case, $|k_a\rangle$ are virtual intermediate states of molecule *a* that emerge in between.

dropped from the graphs and only the orders of the multipoles at the interaction vertices have been retained.

2. Raman scattering to the first interaction order ($M=1$)

Two distinct schemes, *A* and *B*, are possible. In scheme *A*, the photon arrows are attached to different molecules. In all, 12 graphs are relevant, obtained by permuting the photon and intermolecular couplings and by interchanging the arrows. Figure 4 illustrates one typical diagram out of the 12 of scheme *A*. When the usual polarizability approximation holds and the dispersion effects are negligible, we obtain for $l_a=l_b=1$: $U_{2,1}\propto(\Delta\hat{\alpha}_{\mathrm{DID}})_{FI}\propto(\hat{\alpha}_a)_{f_a i_a}(\hat{\alpha}_b)_{f_b i_b}R^{-3}$, where $(\Delta\hat{\alpha}_{\mathrm{DID}})_{FI}$ denotes the dipole-induced dipole (DID) transition polarizability of the pair and $\hat{\alpha}_c$ ($c=a$, b) are the dipole-dipole polarizability tensors of the two molecules. A detailed derivation of these quantities is given in Sec. III. Note that the next order correction is due to the dipole-induced quadrupole (DIQ) polarizability $\Delta\hat{\alpha}_{\mathrm{DIQ}}$ of the pair, with account of W_{21} and W_{12}. In DIQ, $\Delta\hat{\alpha}_{\mathrm{DIQ}}$ scales like R^{-4}.

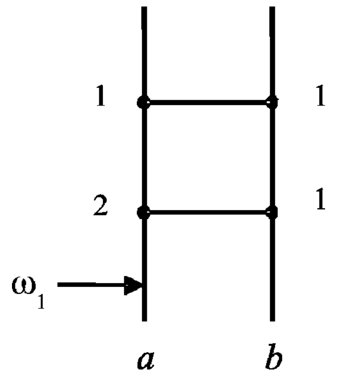

FIG. 3. Same as for Fig. 2, but with the leading second-order intermolecular couplings ($M=2$). The graph is one out of the six possible ones with the photon absorbed by molecule *a*.

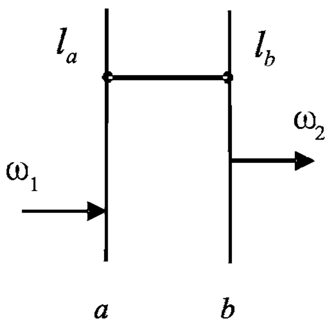

FIG. 4. First-order ($M=1$) collision-induced Raman scattering. The process implicates two molecules, *a* and *b*, and two photons ($N=2$), ω_1 and ω_2. The graph corresponds to one scenario out of the 12 possible ones for $M=1$, and with photons attached to different molecules (multipole-induced multipole mechanism).

In scheme *B*, the photon vertices are placed on the same vertical line, say molecule *b*. There are in all 3! such graphs. Another 3! are obtained when the photon vertices are placed on line *a* and the inductor is molecule *b*. Figure 5 shows a typical graph out of the 6 of scheme *B* with molecule *a* being the inductor. These graphs depict the contributions to $\Delta\hat{\alpha}$ due to the nonlinear (NL) polarization of molecule *b* both by the oscillating field of molecule *a* and by the incident electromagnetic wave. Note that for molecular collisions, the leading term ($l_a=l_b=1$) occurs only when molecule *a* has

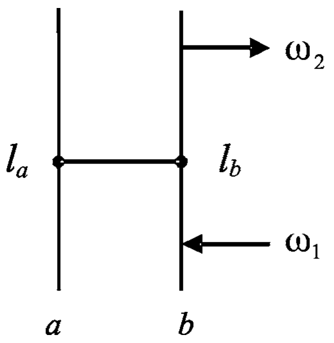

FIG. 5. Same as for Fig. 4, but with both photons interacting with the same molecule (here, *b*). This is a nonlinear mechanism that contributes to the CIRS amplitude and may substantially affect its magnitude. The graph is one out of the six possible ones for $M=1$ and for molecule *a* being the inductor.

a transition dipole moment $(\boldsymbol{\mu}_a)_{f_a i_a}$ and particle b has a transition dipole-dipole-dipole hyperpolarizability $(\hat{\beta}_b)_{f_b i_b}$. Then $(\Delta\hat{\alpha}_{\mathrm{NL}})_{FI} \propto (\boldsymbol{\mu}_a)_{f_a i_a}(\hat{\beta}_b)_{f_b i_b} R^{-3}$.

The next-order term scales like R^{-4} here again. Yet this term consists of two distinct contributions. The first one, $l_a=1$, $l_b=2$, is due to the dipole field gradient and brings into play the dipole-dipole-quadrupole hyperpolarizability $\hat{B}_b$ rather than the dipole-dipole-dipole hyperpolarizability $\hat{\beta}_b$. The second one, namely $l_a=2$, $l_b=1$, is proportional to the matrix elements of the inductor quadrupole $Q_a^{(2)}$ and of the dipole-dipole-dipole hyperpolarizability $\hat{\beta}_b$.

3. Hyper-Raman scattering

Two photons, 1 and 2, are absorbed and a photon, 3, is emitted. Here, in the off-resonance case, the key quantity is the incremental hyperpolarizability $\Delta\hat{\beta}$ of the pair. As before, the diagrams can be ordered as a function of the number of photons that are coupled to one molecule. Again, two distinct schemes, A and B, are possible. In scheme A, one molecule interacts with a pair of photons whereas the other does the same with a single photon. There are in all $3\times 4!=72$ graphs in scheme A. As in the case of the dispersion induction of the dipole moment, it is impossible to factorize $\Delta\hat{\beta}$ in the product of molecular properties.

In scheme B, the three photons are all coupled to the same molecule and a nonlinear polarization of this molecule occurs. Assuming the absorbed photons to be distinguishable (by frequency and/or polarization states) and molecule a to be the inductor, there are $4!=24$ diagrams to generate $\Delta\hat{\beta}$. The leading term scales like $(\boldsymbol{\mu}_a)_{f_a i_a}(\hat{\gamma}_b)_{f_b i_b} R^{-3}$, where $\hat{\gamma}_b$ is the dipole-dipole-dipole-dipole hyperpolarizability.

III. DECOUPLING INTERMOLECULAR PROPERTIES FROM TRANSITION AMPLITUDES

In this section we apply the IST technique to derive vibrational matrix elements of specific incremental electrooptic properties as a function of the rototranslational geometry. Vectors are treated throughout as ISTs of rank 1, and IST ranks are denoted as superscripts in parentheses. Symbol $\Phi_N^{(r)}(j)$ is used to define the ISTs for the field, where j is the number of linearly independent ISTs for given N and rank r $(=0,1,\ldots,N)$ values. Analogously, $\Delta\Gamma_N^{(r)}(j)$ stands for the ISTs of the molecular pair. The derivations are based on the invariant form of $W_{l_a l_b}$ [17] (for definitions and further details, see Appendix A).

In the dipole approximation, the field enters the transition amplitude $U_{N,M}$ via products of the polarization vectors $\mathbf{e}_n = e_n^{(1)}$ $(n=1,2,\ldots,N)$. For one- and two-photon processes, there is a single $\Phi_N^{(r)}(j)$ per rank value, namely $\Phi_1^{(1)}(1)=e_1^{(1)}$ and $\Phi_2^{(r)}(1)=\{e_1^{(1)}\otimes e_2^{*(1)}\}^{(r)}$, with $r=0,1,2$. Rather, for $N\geq 3$, several $\Phi_N^{(r)}(j)$ may appear for a specific rank. Thus, for $N=3$, it is $r=0,1,2,3$, producing seven linearly independent ISTs of the type $\{e_1^{(1)}\otimes\{e_2^{(1)}\otimes e_3^{*(1)}\}^{(l)}\}^{(r)}$, namely, a single IST $(l=1)$, three ISTs $(l=0,1,2)$, two ISTs $(l=1,2)$, and a single IST $(l=2)$, respectively.

Once the decoupling is completed, the transition amplitude (a scalar) can be written as a sum of scalar products between ISTs of the field and ISTs of the pair, $U_N = -\Sigma_{r,j}(\Phi_N^{(r)}(j),(\Delta\Gamma_N^{(r)}(j))_{FI})$. Since for isotropic systems only scalar observables survive, the mean-squared amplitudes (intensities) can be written as a single sum over r. However, for a given value of r (and $N\geq 3$), all different j terms interfere.

Let us now see how $\Delta\Gamma_{N,M}^{(r)}(j)$ are deduced from specific transition amplitudes with the diagrammatic method. Simple guiding examples are given. For the sake of simplicity, only encounters between linear molecules are considered. In this case, the incremental IST of rank r reads

$$(\Delta\Gamma^{(r)}(j))_{FI} = \sum_{\lambda_a\lambda_b\Lambda\lambda} G^{FI}_{\lambda_a\lambda_b\Lambda;\lambda}(R;r;j)\{\{C^{(\lambda_a)}(\Omega_a) \otimes C^{(\lambda_b)}(\Omega_b)\}^{(\Lambda)} \otimes C^{(\lambda)}(\Omega)\}^{(r)}, \tag{2}$$

where Ω_c $(c=a,b)$ designates the orientation of molecule c in the laboratory frame. The expansion of Eq. (2) corresponds to the vector additions $\boldsymbol{\lambda}_a+\boldsymbol{\lambda}_b=\boldsymbol{\Lambda}$ and $\boldsymbol{\Lambda}+\boldsymbol{\lambda}=\mathbf{r}$, and is completely specified by the set of radial functions $G^{FI}_{\lambda_a\lambda_b\Lambda;\lambda}$. Alternatively, the addition scheme $\boldsymbol{\lambda}_b+\boldsymbol{\lambda}=\boldsymbol{\Lambda}_b$ and $\boldsymbol{\Lambda}_b+\boldsymbol{\lambda}_a=\mathbf{r}$ is equally applicable, where $(\Delta\Gamma^{(r)}(j))_{FI}$ is characterized by a new set of radial functions $\widetilde{G}^{FI}_{\lambda_b\lambda\Lambda_b;\lambda_a}$. The latter are linear combinations of $G^{FI}_{\lambda_a\lambda_b\Lambda;\lambda}$over all possible values of Λ and with weighting coefficients proportional to $6j$ symbols. When b is an atom, it turns out that $\lambda_b=0$, $C^{(0)}=1$, and the expansion of Eq. (2) is reduced to a double sum over $\lambda_a(=\Lambda)$ and λ. The simplest case is of course that of two interacting atoms, where the sum is reduced to a single term with $\lambda=r$. Below, only CIA $(r=1)$ and off-resonant CIRS $(r=0,2)$ are considered for which index j can be omitted.

A. Vibrational collision-induced dipole moment

The Mth-order incremental dipole moment can be determined from $U_{1,M} = -(\mathbf{e},(\Delta\boldsymbol{\mu}_M)_{FI})$. For $M=1$, Eq. (1) yields

$$(\Delta\boldsymbol{\mu}_1)_{FI} = -\hbar^{-1}\sum_{k_a}\left(\frac{\langle k_a \mid \boldsymbol{\mu}_a|i_a\rangle\langle f_a f_b|W_{l_a l_b}|k_a i_b\rangle}{\omega_{k_a i_a}-\omega} + \frac{\langle k_a f_b|W_{l_a l_b}|i_a i_b\rangle\langle f_a|\boldsymbol{\mu}_a|k_a\rangle}{\omega_{k_a i_a}+\omega_{f_b i_b}}\right).$$

Upon coupling of $\boldsymbol{\mu}_a = Q_a^{(1)}$ with $Q_a^{(l_a)}$ (the latter quantity enters $W_{l_a l_b}$, see Appendix A), one obtains

$$(\Delta\mu_1^{(1)})_{FI} = -\frac{1}{\sqrt{3}}\sum_{h l_a l_b}(-1)^l A_{l_a l_b}\frac{\Pi_{hl}}{\Pi_{l_a}}\{(P^{(h)}_{1 l_a}(\omega))_{f_a i_a} \otimes (\mathcal{F}_b^{(l_a)}(l_b))_{f_b i_b}\}^{(1)}, \tag{3}$$

where $P^{(h)}_{1 l_a}(\omega)$ is the rank-h irreducible component of the dipole-(2^{l_a}-pole) scattering tensor of molecule a. Particularly, the $l_a=1$ term in Eq. (3) gives the dipole moment that is induced (due to the multipole $Q_b^{(l_b)}$ of molecule b) by the field $\mathcal{E}_b^{(1)} = (-1)^l A_{1 l_b}\mathcal{F}_b^{(1)}(l_b)\Pi_l/\Pi_1$, the latter assumed to be uniform within the volume occupied by molecule a. Similarly, the $l_a=2$ term gives rise to the induction by the gradient of the 2^{l_b}-pole field, whereas the $l_a=3$ term provides the polarization effect of the gradient of the gradient (for a Cartesian tensor approach, see [20]). We point out that Eq. (3) does not in general coincide with the result of classical electrodynamics. Classically, when the rototranslational configuration is fixed, the inductor field $\mathcal{E}_b^{(1)}$oscillates at $\omega_{f_b i_b}$ and polarizes molecule a so that in the uniform field approximation one obtains $(\Delta\boldsymbol{\mu}_1)_{FI} \propto (P_{11}^{(h)}(\omega_{f_b i_b}))_{f_a i_a} (Q_b^{(l_b)})_{f_b i_b} R^{-l_b-2}$. The frequency argument in this result differs from that of quantum mechanics, $\omega \approx \omega_{f_a i_a} + \omega_{f_b i_b}$. For single transitions (i.e., $\omega_{f_a i_a}=0$), the difference between classical and exact results is negligibly small. Rather, for simultaneous transitions, substantial deviations may arise. For instance, when two identical molecules simultaneously undergo the same dipole allowed transition at $\omega_{f_b i_b}=\omega_{f_a i_a}$, a false pole at $k_a=f_a$ appears in the classical resonance term of $(P_{11}^{(h)}(\omega_{f_b i_b}))_{f_a i_a}$, an artifact absent from $(P_{11}^{(h)}(\omega))_{f_a i_a}$in the exact quantum-mechanical treatment.

For linear molecules, the ISTs are proportional to the Racah harmonics $P_{1l_a}^{(h)}=P(h,l_a)C^{(h)}(\Omega_a)$ and $Q_b^{(l_b)} =Q_b(l_b)C^{(l_b)}(\Omega_b)$, where $Q_b(l_b)$ is a constant characterizing the multipole moment of rank l_b and $P(h,l_a)$ is a polarizability invariant. To determine $P(h,l_a)$, one must calculate $P_{1l_a}^{(h)}$ in the molecule-fixed frame. Directing Oz along the molecule-a axis (in this frame, the only surviving component is $C_0^{(h)}=1$), the following nonzero terms are obtained.

(i) $l_a=1$: $P(0,1)=-\sqrt{3}\alpha_a$, $P(2,1)=\sqrt{\frac{2}{3}}\gamma_a$, where $\alpha =\frac{1}{3}\operatorname{Tr}\hat{\alpha}$ and $\gamma=\alpha_{zz}-\alpha_{xx}$ specify the Cartesian tensor $\hat{\alpha}$ of the dipole-dipole polarizability.

(ii) $l_a=2$: $P(1,2)=-\sqrt{\frac{2}{5}}a_{1a}$, $P(3,2)=\sqrt{\frac{3}{5}}a_{3a}$, where $a_{1a} =A_{z,zz}+2A_{x,zx}$ and $a_{3a}=A_{z,zz}-\frac{4}{3}A_{x,zx}$ characterize the dipole-quadrupole polarizability tensor.

By means of these expressions, Eq. (3) allows the determination of the desired set of $\tilde{G}^{FI}_{\lambda_b\lambda\Lambda_b;\lambda_a}$ involved in multipole induction and its first correction.

B. Collision-induced Raman polarization

1. First-order DID

As previously, the photon frequencies ω_1 and ω_2 (and therefore those of the Raman transitions $\omega_{f_a i_a}$ and $\omega_{f_b i_b}$) are assumed to be much lower than the electronic excitation frequencies of the colliding molecules. There are $3!=6$ graphs corresponding to the scenario of a photon 1 absorbed by molecule a and a photon 2 emitted by molecule b (see Fig. 4). Specifically, there are two graphs in which W_{11} lies between the photon couplings; terms proportional to $2(\omega_{k_a i_a}\omega_{k_b i_b})^{-1}$ are so obtained. There are another two graphs in which W_{11} precedes the photon couplings; the resulting terms are proportional to $\omega_{k_a i_a}^{-1}(\omega_{k_a i_a}+\omega_{k_b i_b})^{-1}+\omega_{k_b i_b}^{-1}(\omega_{k_a i_a} +\omega_{k_b i_b})^{-1}=(\omega_{k_a i_a}\omega_{k_b i_b})^{-1}$. Finally, there are two graphs in which W_{11} is the last interaction; they give rise to terms that are identical to those of the preceding situation. We point out that by interchanging the photon vertices, another group of $3!=6$ diagrams is obtained. Mathematically, this interchange is carried out by means of the exchange operator S_{12}—defined via the parity property $S_{12}\Phi_2^{(r)}=(-1)^r\Phi_2^{(r)}$—and results in the factor $[1+(-1)^r]$. Clearly, only ranks $r=0,2$ provide a nonzero contribution. After summation over graphs and subsequent recoupling of ISTs (Appendix B), one obtains

$$(\Delta\alpha^{(r)})_{FI} = 2\sqrt{30}\sum_{sgh}(-1)^s\Pi_{sgh}C_{ij}\{\{(P_{11}^{(g)})_{f_a i_a}\otimes(P_{11}^{(h)})_{f_b i_b}\}^{(s)} \otimes C^{(2)}(\Omega)\}^{(r)}R^{-3},$$

where the vibrational matrix elements of the irreducible static polarizabilities $P_{11}^{(r)}$ were employed, and C_{ij} was used to designate the $\{1,1,r;1,1,2;g,h,s\}$ $9j$ symbol, its entries being sorted as for conventional 3×3 matrices. By means of the above formula, the incremental polarizability for any specific interaction is deduced straightforwardly, and expressions identical to those of the literature [21,22], available for static incremental polarizabilities, are derived. Thus, for isotropic colliders ($h=g=s=0$) and $r=2$, the diagrammatic method provides $(\Delta\alpha^{(2)})_{FI}=2\sqrt{6}(\alpha_a)_{f_a i_a}(\alpha_b)_{f_b i_b}C^{(2)}(\Omega)R^{-3}$, a result coinciding with the pair-atomic anisotropy in the classical DID model. Note that in order to correct this result for dispersion effects, the diagrammatic method remains the only appropriate device.

2. DIQ

In this case $W=W_{21}$ (see Fig. 4). After some algebra, and closely following the steps of Appendix B, one obtains

$$(\Delta\alpha^{(r)})_{FI} = 2\sqrt{105}\sum_{sgh}(-1)^s\Pi_{sgh}C_{ij}\{\{(P_{12}^{(h)})_{f_a i_a}\otimes(P_{11}^{(g)})_{f_b i_b}\}^{(s)} \otimes C^{(3)}(\Omega)\}^{(r)}R^{-4},$$

where $P_{12}^{(h)}$ ($h=1,3$) denotes the irreducible components of the dipole-quadrupole static polarizability tensor $\hat{A}$. The entries of the $9j$ symbol, sorted in the way explained above, are $\{1,1,r;2,1,3;h,g,s\}$.

When a is a linear molecule and b is an isotropic particle ($g=0$),

$$(\Delta\alpha^{(0)})_{FI} = 2\sqrt{21}(\alpha_b)_{f_b i_b}(a_{3a})_{f_a i_a}\{C_a^{(3)}\otimes C^{(3)}\}^{(0)}R^{-4},$$

$$(\Delta\alpha^{(2)})_{FI} = -\frac{6\sqrt{14}}{5}(\alpha_b)_{f_b i_b}[(a_{1a})_{f_a i_a}\{C_a^{(1)}\otimes C^{(3)}\}^{(2)} - (a_{3a})_{f_a i_a}\{C_a^{(3)}\otimes C^{(3)}\}^{(2)}]R^{-4}.$$

3. Nonlinear dipole-field induction

In this case, the vibrating dipole of molecule a is a source of the internal field. For a centrosymmetric particle b, the relevant interaction is due to the dipole-quadrupole coupling W_{12}. Only six diagrams contribute because both photon lines should be attached to line b (see Fig. 5). We obtain (Appendix C)

$$(\Delta\alpha^{(r)})_{FI} = \sqrt{21}\sum_{s} \frac{(-1)^{s}\Pi_{s}}{\Pi_{r}}\{(B_{b}^{(s)})_{f_b i_b} \otimes (\mathcal{F}_{a}^{(2)})_{f_a i_a}\}^{(r)} R^{-4}, \tag{4}$$

where $(B_{b}^{(s)})_{f_b i_b}$ (defined therein) designates the matrix elements of the irreducible component of the dipole-dipole-quadrupole static hyperpolarizability tensor $\hat{B}$ of b. For atomic perturbers, only the isotropic component $B^{(0)}=\sqrt{\frac{15}{2}}B$ appears, with $B=B_{ZZ,ZZ}$. In the "atom-linear molecule" case, the general expression of Eq. (4) is reduced to

$$(\Delta\alpha^{(0)})_{FI} = 0,$$

$$(\Delta\alpha^{(2)})_{FI} = \frac{3}{2}\sqrt{14} B_{b} (\mu_{a})_{f_a i_a} \{C_{a}^{(1)} \otimes C^{(3)}\}^{(2)} R^{-4},$$

and the incremental polarizability turns out to be entirely anisotropic. This nonlinear polarizability induction mechanism had been overlooked in the previous classical treatment [8].

IV. CONCLUSIONS

We developed a diagrammatic approach to specify, to sort, and to depict the interaction mechanisms between the electromagnetic field and a pair of weakly interacting molecules. We provided evidence of the occurrence of a nonlinear polarization mechanism—absent from any previous studies—whose contribution to collision-induced Raman bands of certain molecules is expected to be substantial. Our method turned out to be a powerful device for deriving the long-range part of incremental electro-optic properties of a pair of molecules for any collision-induced process. Given that obesrvations of either CIA, CIRS, or CIHRS spectra by many practically important molecular gases benefit nowadays from high accuracy measurements, electro-optic properties can be experimentally accessed, and their link to our method advances the cause of fundamental physics and of atmospheric spectroscopy. Another advantage of our description is that it opens the door to nonempirical calculations of collision-induced hyperpolarizabilities, quantities largely unknown in today's state of the art. Work is in progress in our groups.

ACKNOWLEDGMENTS

This work was done as a collaborative project between the University of Angers and the Saint Petersburg State University. The authors acknowledge support from the Laboratoire POMA, UMR CNRS 6136.

APPENDIX A: INTERACTION ENERGY

The interaction energy between multipoles $Q_{a}^{(l_a)}$ and $Q_{b}^{(l_b)}$ reads

$$W_{l_a l_b} = A_{l_a l_b} (-1)^{l} \Pi_{l} \{Q_{a}^{(l_a)} \otimes \mathcal{F}_{b}^{(l_a)}(l_b)\}^{(0)},$$

where $\mathcal{F}_{b}^{(l_a)}(l_b)=\{Q_{b}^{(l_b)} \otimes C^{(l)}(\Omega)\}^{(l_a)} R^{-l-1}$ and $\{A^{(r)} \otimes B^{(s)}\}^{(t)}$ stands for convolution of two ISTs of ranks r and s into an IST of rank t; $A_{l_a l_b}=(-1)^{l_b}\sqrt{(2l)!/(2l_a)!(2l_b)!}$; $\Pi_{ab\cdots c}=\sqrt{(2a+1)(2b+1)\cdots(2c+1)}$; $C^{(l)}$ is the Racah spherical harmonics [18] of rank $l=l_a+l_b$; $\mathbf{R}=(R,\Omega)=\overrightarrow{ab}$.

APPENDIX B: DID

The transition amplitude reads

$$U_{2,1} = - S_{D}\sqrt{6}\sum_{k_a k_b} \hbar^{-2} \omega_{k_a i_a}^{-1} (\omega_{k_a i_a} + \omega_{k_b i_b})^{-1} \times ((\mu_{a}^{(1)})_{k_a i_a}, e_{1}^{(1)})((\mu_{b}^{(1)})_{k_b i_b}, e_{2}^{*(1)}) \times (\{(\mu_{a}^{(1)})_{f_a k_a} \otimes (\mu_{b}^{(1)})_{f_b k_b}\}^{(2)}, C^{(2)}(\Omega)),$$

where S_D has formally accounted for the summation over graphs and where, for the sake of simplicity, only the graph of Fig. 4 has been explicitly considered. The next two steps consist in decoupling the polarization factor $\Phi_{2}^{(r)}$ from $((\mu_{a}^{(1)})_{k_a i_a}, e_{1}^{(1)})((\mu_{b}^{(1)})_{k_b i_b}, e_{2}^{*(1)})$ and in rearranging the result so that irreducible products $\{\mu_{c}^{(1)} \otimes \mu_{c}^{(1)}\}^{(t)}$ $(c=a,b)$ are formed (for further details, see [18]).

APPENDIX C: NONLINEAR DIPOLE

Upon decoupling of the polarization factor, one obtains

$$(\Delta\alpha^{(r)})_{FI} = S_{D}\sqrt{15}\sum_{k_b n_b} \hbar^{-2} \omega_{k_b i_b}^{-1} \omega_{n_b i_b}^{-1} \frac{\Pi_{3}}{\Pi_{2}} \{(\mu_{b}^{(1)})_{k_b i_b} \otimes (\mu_{b}^{(1)})_{n_b k_b}\}^{(r)} ((Q_{b}^{(2)})_{f_b n_b}, (\mathcal{F}_{a}^{(2)}(1))_{f_a i_a}) R^{-4}.$$

Straightforward recoupling of the right-hand side results in Eq. (4), with

$$(B_{b}^{(s)})_{f_b i_b} = S_{D}\sum_{k_b n_b} \hbar^{-2} \omega_{k_b i_b}^{-1} \omega_{n_b i_b}^{-1} \{\{(\mu_{b}^{(1)})_{k_b i_b} \otimes (\mu_{b}^{(1)})_{n_b k_b}\}^{(r)} \otimes (Q_{b}^{(2)})_{f_b n_b}\}^{(s)}.$$

[1] L. Frommhold, *Collision-induced Absorption in Gases* (Cambridge University Press, Cambridge, 1993).

[2] L. Frommhold, Adv. Chem. Phys. **46**, 1 (1981).

[3] *Molecular Cryospectroscopy*, edited by M. O. Bulanin, Advances in Spectroscopy Vol. 23, edited by R. J. H. Clark and R. E. Hester (Wiley & Sons, Chichester, 1995), Chap. 6.

[4] S. M. El-Sheikh, G. C. Tabisz, and A. D. Buckingham, Chem. Phys. **247**, 407 (1999).

[5] V. Teboul, Y. Le Duff, and T. Bancewicz, J. Chem. Phys. **103**, 1384 (1995).

[6] O. Gaye, M. Chrysos, V. Teboul, and Y. Le Duff, Phys. Rev. A **55**, 3484 (1997).

[7] K. Novicka, T. Bancewicz, J-L. Godet, Y. Le Duff, and F. Rachet, Mol. Phys. **101**, 389 (2003).
[8] R. D. Amos, A. D. Buckingham, and J. H. Williams, Mol. Phys. **39**, 1519 (1980).
[9] P. Kaatz and D. P. Shelton, Mol. Phys. **88**, 683 (1996).
[10] X. Li, K. L. C. Hunt, J. Pipin, and D. H. Bishop, J. Chem. Phys. **105**, 10954 (1996).
[11] W. Głaz, T. Bancewicz, and J-L. Godet, J. Chem. Phys. **122**, 224323 (2005).
[12] J. F. Ward, Rev. Mod. Phys. **37**, 1 (1965).
[13] R. Wallace, Mol. Phys. **11**, 457 (1966).
[14] J. H. Christie and D. J. Lockwood, J. Chem. Phys. **54**, 1141 (1971).
[15] P. N. Butcher and F. Cotter, *The Elements of Nonlinear Optics* (Cambridge University Press, Cambridge, 1990).
[16] D. P. Craig and T. Thirunamachandran, *Molecular Quantum Electrodynamics* (Dover, Mineola, NY, 1998).
[17] C. G. Gray and K. E. Gubbins, *Theory of Molecular Fluids* (Clarendon Press, Oxford, 1984).
[18] D. A. Varshalovich, A. N. Moskalev, and V. K. Khersonskii, *Quantum Theory of Angular Momentum* (World Scientific, Singapore, 1988), Chap. 3.
[19] Notation $(\mathcal{A})_{k'k}$ stands for matrix element $\langle k' | \mathcal{A} | k \rangle$ of operator $\mathcal{A}$.
[20] A. D. Buckingham, Adv. Chem. Phys. **12**, 107 (1967).
[21] M. O. Bulanin and A. P. Kouzov, Opt. Spectrosc. **53**, 266 (1982).
[22] M. Kazmerczak and T. Bancewicz, J. Chem. Phys. **80**, 3504 (1984).